

Finite Element Analysis of an Aircraft Wing Under Drag Load

Tye Cameron-Robson (Student No: C2038216)

MEng in Advanced Mechanical Engineering, Cardiff School of Engineering, Cardiff University.

Abstract:

This report presents a finite element analysis of a simplified two-dimensional aircraft wing subjected to drag loading. A solver was developed, capable of handling both 4-noded and 8-noded quadrangular element meshes. The analysis focuses on the effect of backward sweep (θ) and dihedral (ϕ) angles on the wing's maximum principal stresses. Key findings demonstrate the solver's robustness in visualising stress distributions and identifying trends related to varying geometries, providing valuable insights for structural optimisation [1]. The report highlights how orthotropic material properties influence stress distributions, and results are visualised using Paraview for clarity. Future work could explore extending this solver to three-dimensional models, incorporating additional aerodynamic loads such as lift.

1. Introduction:

Aircraft wings experience complex aerodynamic forces during flight, with drag being a critical load that influences their structural integrity. In this study, the two-dimensional geometry of a backward-swept aircraft wing is simplified to explore the effects of the backward sweep angle (θ) and dihedral angle (ϕ) on the maximum principal stress. The wing's semi-span length is fixed with a length ratio of $L1:L2 = 1:3$, while θ and ϕ are varied between 60° and 90° . The analysis is conducted under the following assumptions:

- Drag force acts in the negative y direction.
- Material properties are assumed to be orthotropic [4].
- The semi-span ($L1 + L2$) is fixed, with a ratio of $L1:L2 = 1:3$.
- The length of $L1$ is fixed at 8m, and the wing area is kept constant at 250m^2 .

This study quantifies the effect of geometric parameters on wing stress distributions. This analysis aims to provide detailed visualisations of the results, which will assist in design optimisation for minimising stress concentrations. The outcomes are critical for ensuring both structural safety and aerodynamic efficiency [5].

2. Methodology

Finite Element Solver Overview

The solver is designed with modular functions for 4-noded and 8-noded quadrangular elements, including:

1. Mesh generation based on parameters ($L1, \theta, \phi$).
2. Quadrature integration to compute the stiffness matrix, strain-displacement relations, and force weightings at each quadrature point.
3. Stress calculations for principal stresses, Von Mises stress, and shear stress.
4. Assembly of the stiffness matrices into a sparse global matrix, with Dirichlet boundary conditions for $x=0$.
5. Strain calculations post-boundary conditions, with results prepared for Paraview visualisation.
6. Differential evolution for geometry optimisation, using multiprocessing to efficiently explore material property variations with a population size of 10 and a maximum 25 iterations (for a total of 25,000 solutions across the various material simulations).

Mesh Generation & Refinement

The solver refines meshes based on user-defined minimum element size. Finer meshes capture stress gradients near the wing root [2]. The wingMesher function calculates the area, plots 5 coordinates, and refines the mesh in a tiered structure, focusing on fixed support vertices (points 1 and 5) and the most acute angle vertex (point 3).

Finite Element Procedure

The mesh is processed using Gmsh, leveraging vectorised operations for efficiency where appropriate. For each element, the x and y node coordinates are extracted using the pyvista connectivity matrix. Quadrature integration calculates shape function derivatives, element strain-displacement (Be) matrix, and stiffness matrix using B^TDB matrix multiplication [6]. Numpy's einsum integrates the Be and Ke matrices across quadrature points. The global stiffness matrix is constructed, Dirichlet boundary conditions and drag force are applied [2], and stress calculations (principle and Von Mises) are stored for Paraview visualisation.

Material Properties

The wing material is orthotropic, with typical values for elasticity modulus (E1, E2), Poisson's ratio (ν_{12}), and shear modulus (G12) in the following ranges:

- E1 = 130-230 GPa
- E2 = 5-10 GPa
- $\nu_{12} = 0.3$
- G12 = 4-8 GPa

These properties are varied to analyse their effects on geometry and stress gradients.

Optimisation Procedure

A differential evolution algorithm from SciPy optimises the wing geometry (θ , ϕ) for various material properties. Using Python's multiprocessing library, simulations run in parallel on multiple CPU cores with a maximum of 25 iterations, a population size of 10, and convergence tolerance of 2.5%. A coarse mesh (0.4 minimum) is used to avoid local minima, and the weighted criteria (0.75 Von Mises vs. 0.25 shear stress) guides optimisation [3]. The optimal geometry is refined with a finer mesh, and results (angles, stresses, strains, material properties) are stored for post-processing [2].

Visualisation

Results are exported to Paraview for stress and deformation analysis, with sparse matrix plots used to verify Dirichlet boundary condition functionality [7].

3. Results

Stress Visualisations

The visualisation of stress distributions shows the effect of the angle parameters (θ and ϕ) on principal stresses. In the analysis of backward-swept wings, larger values of θ resulted in noticeable stress concentrations at the wing root, a consequence of increased bending moments. In contrast, the application of ϕ , specifically dihedral angles, was found to reduce stress concentrations, enhancing the structural load redistribution of the wing.

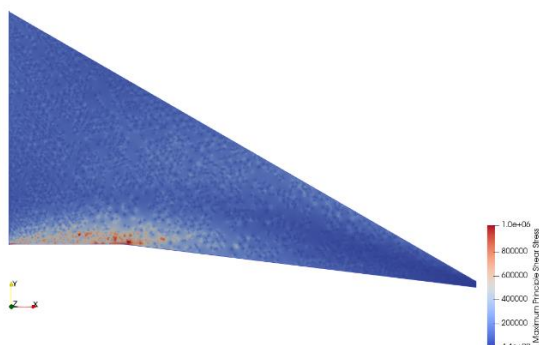
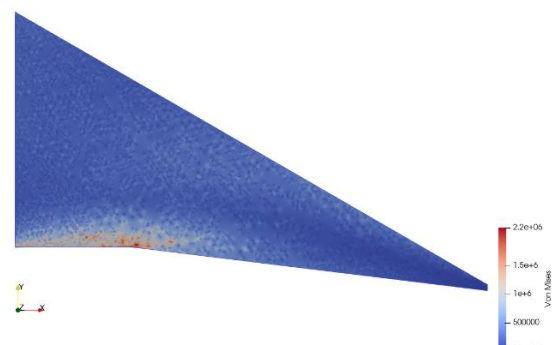


Figure _a: Principal Shear Stress Distribution



Figure_b: Von-Mises Stress Distribution

Figures X and Y display the principal and Von-Mises stress distributions for the optimised wing configuration. Both profiles show peak stresses near the dihedral vertex, with a diminishing trend along the span, attributed to the uniaxial compression predominating in the wing's stress state. This trend reflects the minimal contributions from shear and normal stresses in the x-direction due to material properties and the direction of the applied drag force.

Mesh Comparison: 4-Noded vs. 8-Noded Elements

A comparison of 4-noded and 8-noded elements reveals a trade-off between computational efficiency and accuracy. While the 8-noded elements provide greater accuracy in gradients and values near critical regions, they result in a ~35% increase in computational time. This emphasises the need to balance precision with computational efficiency during design.

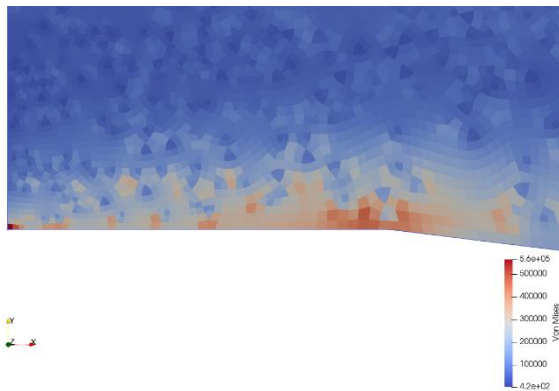


Figure _: 4 Noded Root & Dihedral Region

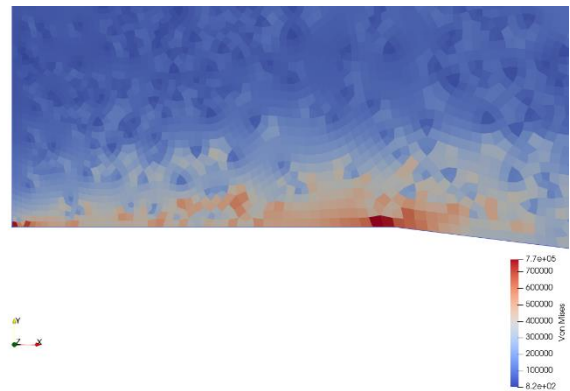


Figure _: 8 Noded Wing & Dihedral region

Stress Concentration Trends

The maximum principal stresses (σ_{xx} , σ_{yy}) were analysed as a function of θ and ϕ , and visualised in 3D surface plots.

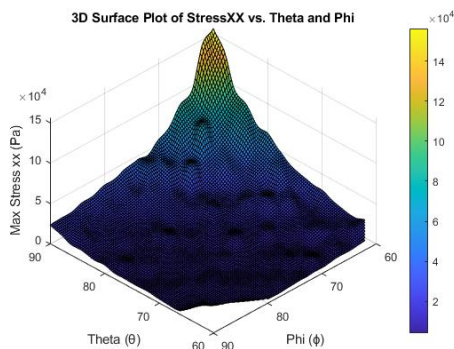


Figure _: The Effect of θ and ϕ with maximum σ_{xx}

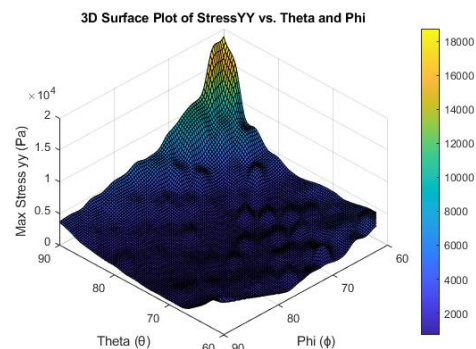


Figure _: The Effect of θ and ϕ with maximum σ_{yy}

Figures C and D segregate the stress loads in the x and y directions. The trends show that the σ_{xx} stress is significantly greater than σ_{yy} , owing to the uniaxial loading conditions and material properties. The interplay between θ and ϕ demonstrates the influence of geometric parameters on stress distribution, with the optimal region occurring at minimal θ and maximal ϕ .

Optimised Wing Geometry for Material Selections

The optimisation process evaluated 45 material-property combinations, identifying configurations that minimised stress. The optimal parameters were found to be $E1 = 205$ GPa, $E2 = 10$ GPa, and $G12 = 4$ GPa, with $\theta = 60.01^\circ$ and $\phi = 83.01^\circ$, yielding a maximum Von Mises stress of 0.91 MPa and principal shear stress of 0.43 MPa.

E1 (GPa)	E2 (GPa)	G12 (GPa)	Theta (°)	Phi (°)	Max VM (MPa)	Max Principle Shear (MPa)
205.00	10.00	4.00	60.01	83.01	0.91	0.43
130.00	10.00	8.00	63.31	86.38	0.99	0.47
130.00	7.5.00	6.00	60.53	83.60	1.00	0.47
180.00	10.00	6.00	63.43	87.18	1.03	0.49
155.00	10.00	8.00	63.30	86.35	1.04	0.49

Table _: Best 4 Optimal Material Properties & Angle Parameters (Ascending)

Material Behaviour

Table X shows that higher material stiffness (E1, E2) correlates with increased stress magnitudes, particularly in Von-Mises stress, indicating that stiffer materials may fail at lower stress levels. Displacement analysis shows minimal deformation, contributing to stability. However, further evaluation using criteria such as fatigue or fracture mechanics is necessary for a complete assessment of structural integrity.

Sparse Matrix Visualisations

Sparse matrix visualisations of the global stiffness matrix reveal trends in stress distributions.

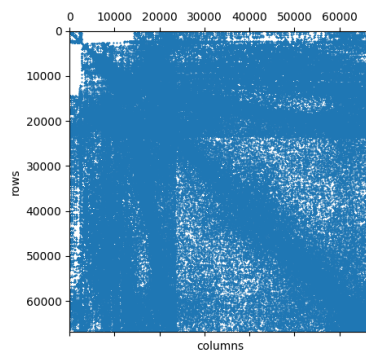


Figure _: Global Stiffness Matrix before Dirichlet Boundary Conditions

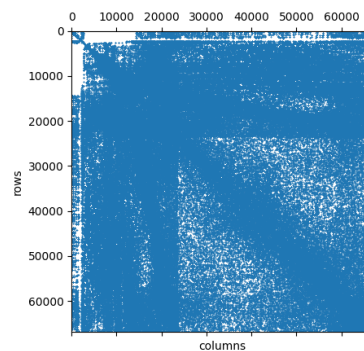


Figure _: Global Stiffness Matrix after Dirichlet Boundary Condition

The sparse matrix plots indicate regions with minimal strain, where the geometry of the wing effectively carries loads. Dense regions near the root, however, highlight areas that may require additional structural reinforcement.

Eigen Value Analysis

Eigenmode analysis reveals how the wing deforms under loading, with each eigenvalue reflecting the natural frequency of the corresponding mode.

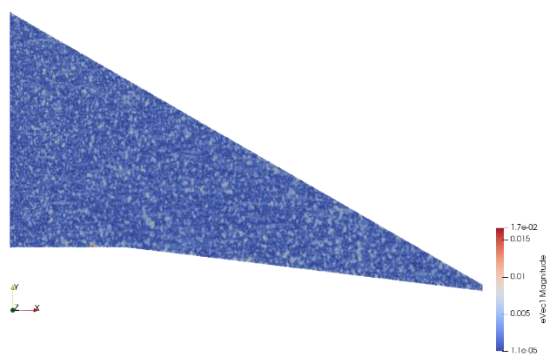


Figure _: First Bending Mode Eigen Vector

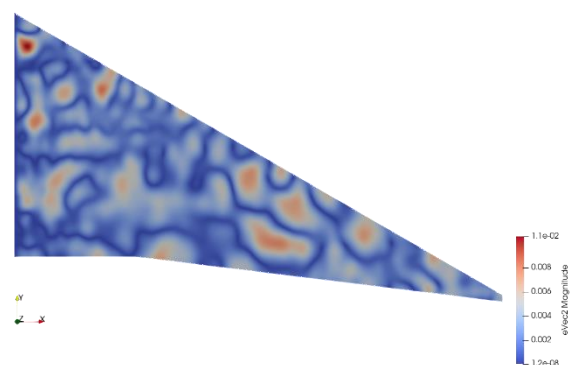


Figure _: First Torsional Mode Eigen Vector

The first bending mode, shown in **Figure X**, is crucial for understanding the wing's response to aerodynamic loads. If this mode resonates with aerodynamic forces, it could lead to excessive deflection and compromise the wing's performance. Similarly, the first torsional mode (Figure Y) highlights the twisting behaviour under aerodynamic moments, which could lead to instability if resonant conditions are met.

4. Discussion & Future Work:

This study examined how variations in the backward sweep angle (θ) and dihedral angle (ϕ) affect stress distribution across the wing structure. Increasing θ results in greater stress concentrations at the wing root due to larger bending moments. In contrast, a higher value of ϕ redistributes stresses more efficiently towards the dihedral, improving the wing's overall structural integrity. A combination of minimal θ and larger ϕ emerges as optimal for minimising a wing's stress concentrations.

The study also explored the impact of material properties on stress magnitudes. The elasticity moduli ($E_{1,2}$) potentially lead to reduced stress levels, especially in Von Mises stress, while also increasing susceptibility to failure at lower stress thresholds. A discontinuity between elasticity moduli and optimal results requires further investigation. This uncertainty emphasises the importance of carefully selecting materials that balance drag capacity with other structural performance metrics. Furthermore, the observed outliers in stress magnitudes particularly incite studies into fatigue and fracture in real-world applications.

The trade-off between computational efficiency and accuracy was highlighted in the comparison of 4-noded and 8-noded elements. While 8-noded elements offer greater accuracy in predicting stress, especially in high-stress regions, they lead to an increase in computational time by 35%. This necessitates careful consideration of accuracy and computational cost when performing large-scale simulations or real-time applications. However, for critical analyses, the accuracy provided by 8-noded elements remains indispensable.

The solver efficiency leaves room for improvement regarding program efficiency and calculation accuracy. Further vectorised operations can be leveraged for maximum processor utilisation, and rather than averaging values over elements, the stress values could be converted to finer gradients utilising the quadrature point calculations.

The optimisation of wing geometry and material properties was performed using a differential evolution algorithm. This process identified configurations that reduced principal and Von Mises stress. However, certain simulations failed due to mesh-related issues or matrix singularities, suggesting that further refinement in mesh generation and solver procedures is necessary. The optimisation results underscore the significant influence of geometry and material on the wing's structural performance, although some variation between results and expectations can be attributed to the minimal population size and forced iteration limit necessitated by the high computational load.

The report touches on Eigenvalue analysis, visualising the wing's bending and torsional modes which would lead to instability if resonant conditions occurred. To prevent performance issues related to resonance, it is essential that the wing's natural frequencies are sufficiently distanced from those expected during flight. Modifying the wing's geometry or stiffness may be necessary to shift natural frequencies, but this effect was not measured within the report.

Future research should focus on extending the current analysis to simulate dynamic loading and the aerodynamic forces experienced during flight. Incorporating failure criteria like fatigue and fracture mechanics would improve the model's realism. Additionally, developing a three-dimensional solver would provide accurate representations of larger aircraft structures and their performance in real-world conditions, and the eigenvalue design considerations would be vital to ensure reliability of real-world applications.

In conclusion, the FEA solver has proven effective in optimising wing geometry and material properties, leading to reduced stress concentrations. The study highlights geometry, material selection, and boundary conditions to be crucial in designing wings with high performance and structural integrity.

5. Bibliography:

- [1] K. J. Bathe, *Finite Element Procedures*. Prentice Hall, New Jersey, USA, 1996.
 - [2] O. C. Zienkiewicz and R. L. Taylor, *The Finite Element Method*, Fourth. London: McGraw-Hill, 1991.
 - [3] M. Ainsworth and J. T. Oden, *A posteriori error estimation in finite element analysis*, vol. 37. John Wiley & Sons, 2011.
 - [4] Almeida, F. and Awruch, A. (2015). *Aeroelastic analysis of wings with isotropic and orthotropic materials in compressible flow*. Journal of the Brazilian Society of Mechanical Sciences and Engineering, 38(4), 1087-1102.
 - [5] Zhang, S. and Mikulich, M. (2021). *Parametric cad modelling of aircraft wings for fea vibration analysis*. Journal of Applied Mathematics and Physics, 09(05), 889-900.
 - [6] Mousavi, M. and Sukumar, N. (2010). *Generalized gaussian quadrature rules for discontinuities and crack singularities in the extended finite element method*. Computer Methods in Applied Mechanics and Engineering, 199(49-52), 3237-3249.
 - [7] Lee, H. and Reichl, L. (2010). *r-matrix theory with dirichlet boundary conditions for integrable electron waveguides*. Journal of Physics a Mathematical and Theoretical, 43(40), 405303.
-

Self-assessment Form (1 page max):

Assessment of one's own overall performance: (9 out of 10)

Professional skills & behaviour: (9 out of 10)

Justification/Evidence:

Attended every lecture and laboratory session without fail.
Took initiative to organise most group meetings and ensured regular communication within the team.
Worked on the solver consistently every week, ensuring no progress was delayed.
Understood and applied key concepts moderately well and provided regular updates on personal progress.
Supported group members by explaining key concepts, breaking down coding problems, and simplifying solutions during weekly meetings.
Made efforts to distribute workloads, although challenges with team engagement limited full implementation.
Hence balanced intense workload independently.
Maintained group integrity by updating every new addition to the solver in teams.

Engineering Excellence: (9 out of 10)

Justification/Evidence:

Contributed to the initial breakdown of the problem and rough planning of the project.
Integrated advanced numerical methods into the solver to enhance its accuracy and functionality.
Regularly communicated with both the team and external groups to benchmark results and troubleshoot effectively.
Successfully resolved all encountered technical problems and demonstrated resilience in overcoming troubleshooting challenges.

Coding & Implementation: (9 out of 10)

Justification/Evidence:

Developed the submitted solver entirely through personal effort, relying on both external sources and course materials.
Took the lead in coding as other group members had limited experience with programming.
Group meetings primarily involved progress updates and conceptual discussions, with coding tasks largely completed independently.

Assessment of group member's overall performance:

M1: Dani Unzu (7 out of 10)

Dani attended every group meeting and laboratory session, contributing consistently where possible (trigonometric coordinate system, followed the lab content but took longer to grasp it than the module necessitated).

Demonstrated a good understanding of concepts and provided valuable input during discussions.
While contributions to coding and numerical methods were limited, Dani actively participated in troubleshooting and reviewing results.

M2: Hussain Shafqiat (5 out of 10)

Hussain did not set up the required environment until during the penultimate lab session, despite weekly meetings and discussions organised.
Participation in coding and implementation was minimal, despite frequent guidance from other team members.
Contributed to group discussions but lacked initiative in course engagement and tackling technical challenges independently.